Preprints.org

Article

Thermo-Mechanical Behaviour of Green Sandwich Structures for Building and Construction Applications

Forhad Hossain , Md Arifuzzaman * , Md Shariful Islam , Md Mainul Islam

Article

Thermo-Mechanical Behaviour of Green Sandwich Structures for Building and Construction Applications

Forhad Hossain [1], Md Arifuzzaman [1,*], Md Shariful Islam [1] and Md Mainul Islam [2]

[1] Department of Mechanical Engineering, Khulna University of Engineering & Technology, Khulna 9203, Bangladesh; Email: forhadakib101@gmail.com (F.H.); arif48@me.kuet.ac.bd (M.A.); msislam@me.kuet.ac.bd (M.S.I.)

[2] School of Engineering and Centre for Future Materials, University of Southern Queensland, Toowoomba, Queensland 4350, Australia.

* Correspondence: arif48@me.kuet.ac.bd

Abstract: In this work, three different types of sandwich structures were manufactured using Formica sheet (a paper-based sheet) as skin and perlite/sodium silicate foam as core with/without the paper honeycomb. The sandwich structures were fabricated by attaching Formica sheets on both sides of the honeycomb, perlite/sodium silicate foam, and perlite/sodium silicate foam-filled honeycomb core panels. The flexural characteristics were studied by a three-point bending test and the thermal conductivity was measured using Lee's thermal conductivity apparatus. The results demonstrated a significant improvement in flexural properties, including core shear stress, facing stress, bending stress, and energy absorption, when incorporating the paper honeycomb reinforcement. The thermal conductivity and flexural properties were found to be well-compatible with the existing building materials for similar applications in the literature. The failure investigation revealed that the sandwiches with paper honeycomb only prematurely failed due to core buckling, whereas the foam-filled honeycomb core-based sandwiches were able to sustain higher loads, exhibiting material failures such as core shear failure, skin rapture, and delamination. It is found that the foam-filled paper honeycomb sandwich structures can withstand higher bending loads compared to foam core-based and paper honeycomb-based sandwich structures. These developed sandwiches offer potential as green materials due to the characteristics of their constituent materials and can find valuable applications in the building thermal insulation.

Keywords: perlite composite-filled paper honeycomb sandwich; thermal insulation board; green sandwich structure; flexural properties; thermal conductivity

1. Introduction

Expanded perlite is a lightweight material that is used extensively because of its appealing chemical and physical characteristics. The raw perlite particles obtained from the obsidian typically increase in volume by 5 - 20 times when rapidly heated to a temperature of 900 °C to 1200 ºC [1]. They are used in construction industries because of their low bulk density [2] and attractive properties. Expanded perlite particles are environment-friendly and chemically inert while possessing strong heat and fire resistance, low thermal conductivity, and good sound insulation characteristics [3-5]. The uses of expanded perlite particles for the development of building materials were covered extensively in a review by Rashad [6]. Expanded perlite particle-based building boards were studied by many researchers, including fiber/asphalt coated perlite building boards by Miscall and Rahr [7]; mineral board by Sherman and Cameron [8]; perlite/starch foam by Shastri and Kim [9]; gypsum/perlite composite by Vimmrova [10] and Karua and Arifuzzaman [11]; perlite/sodium silicate board by Arifuzzaman and Kim [12-15] Adhikary et al. [16], Karua and Arifuzzaman [17], Takey et al. [18], Tian et al. [19], Abir et al. [20], etc. Perlite/sodium silicate foam may be an alternative to the gypsum board because of its lightweight, high strength-to-weight ratio, and better thermal and acoustic insulation. The concentration of sodium silicate in perlite-based foams plays a vital role in

the physical and mechanical properties of the boards. It was found from the literature that the density, compressive and flexural strength of expanded perlite board increases linearly with increasing the concentration of sodium silicate [14], [12], [19]. The effect of sodium silicate binder and compaction ratio on the mechanical properties of perlite-based building boards was broadly studied by Arifuzzaman and Kim [12, 13]. One of the important characteristics of the perlite/sodium silicate composite foam is that the failure of the perlite/sodium silicate panels initiates on the specimen's tensile side [13] during flexural loading causing a lower load-bearing capacity and toughness. However, they found that the failure side was shifted to the mid-plane of the flexural specimen, and the load-bearing capacity was increased by roughly 3–7 times with Brown paper reinforcement as the skin for the sandwich structure [21]. So, sandwiching perlite/sodium silicate composite foams with various skins would influence the flexural properties based on the skin material properties.

Paper honeycomb sandwich panels have been used to package large-scale goods, furniture, building materials, and other things due to their lightweight, high strength, and cushioning characteristics [22-24]. The paper honeycomb sandwich structures for building applications were studied in the past [25-28]. For example, Shahbazi et al. [25] investigated a sandwich structure made of flax fiber-reinforced Portland cement and kraft paper honeycomb as face sheet and core material respectively. The flexural and thermal properties were found to be compatible with traditional gypsum boards. Kadir et al. [27] examined the effective method for finding the ideal arrangement of kraft paper honeycombs and the effects of paper density, cell wall thickness, and honeycomb cell size on specific energy absorption and specific compressive strength. The findings showed that all parameters had a discernible impact but the width of the cell wall had the greatest impact on the functionality of kraft paper honeycomb. The effects of foam filling on the behavior and failure of sandwich panels made of a paper honeycomb core are limited. Fu and Sadeghian [26] found that filling the paper honeycomb core cells with polyurethane foam increased the load-bearing capacity of the sandwiches [26]. Kadir et al. [27] also used low-density polyurethane to fill the kraft paper honeycomb cells and the findings showed that adding polyurethane foam to the kraft paper honeycomb helped reinforce the cell walls, which in turn increased the honeycomb's capacity to absorb energy and the peak force. Therefore, filling the paper honeycomb core cells with lightweight expanded perlite foams would benefit load-bearing capacity and toughness.

The face sheet material has a significant impact on the flexural properties of the sandwich structure. For example, Safarabadi et al. [29] studied the Nomex honeycomb core with glass-epoxy face sheet sandwich panels buckling behavior for both bare and foam-filled cores. They reported that the presence of foam raised the crucial buckling load and the characteristics of the face sheets had a greater influence on the buckling behavior and energy absorption or toughness of the composite panel based on their experimental and numerical findings. Sandwich structures made of the expanded perlite-based core are limited in the literature. Arifuzzaman and Kim [21] studied the flexural behavior of expanded perlite/sodium silicate core-based sandwich structures using Brown paper as skin. Recently, Sarkar et al. [30] and Hossain et al. [31] investigated sandwich structures using jute fiber-reinforced epoxy composite as skin and expanded perlite/epoxy and expanded perlite/sodium silicate cores respectively. Formica sheets made of high-graded craft paper may be a good candidate for the skin of the perlite/sodium silicate core-based sandwich structure because of their widespread use in the furniture industries and building interior decoration.

In this work, Novel green sandwich structures were formulated using expanded perlite/sodium silicate foam, paper honeycomb, and perlite/sodium silicate foam-filled paper honeycomb cores with Formica sheet as skin. The flexural and thermal behavior of the manufactured composites were investigated and compared with similar existing building materials in the literature.

3. Materials and Method

3.1. Materials

For manufacturing perlite foam-filled honeycomb sandwich structures, the honeycomb structure was made using Kraft paper, and the cells of the paper honeycomb structure were filled

with perlite/sodium silicate composite foam. The Formica sheet was used as the skin of sandwich structures which was bonded to the core using a synthetic resin adhesive (Fevicol SH). A schematic of the sandwich structure of concern is shown in **Figure 1**.
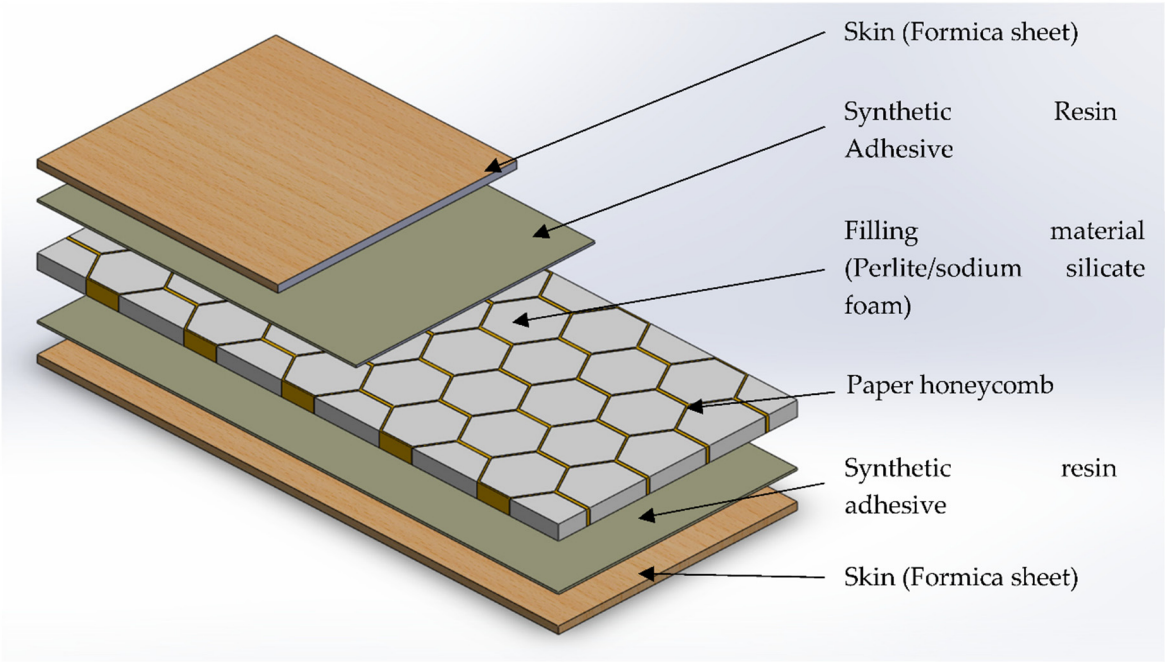

Figure 1. A schematic view of the honeycomb sandwich structure considered in this study.

Kraft liner paper with an average thickness of 0.49 mm was purchased from the local market. Skin glossy-finished Formica sheet 'Formica & Ebonite (HPL) 717' of thickness 0.50 mm (Super Formica & Lamination Limited) was bought from a local supplier. According to the manufacturer, the raw material of the Formica sheet is high-graded craft paper, phenol formaldehyde, and melamine formaldehyde resin. The sheet is scratch-resistant and has firm, slick surfaces. Multiple layers of impregnated paper are fused under high temperatures and pressure to manufacture Formica sheets. It is tough, long-lasting, and non-toxic to humans. The tension test of the Formica sheet was conducted in a Universal testing machine (Shimadzu AGX 300kNV, Japan) at a crosshead speed of 5 mm/min to determine the tensile properties. The coupon specimen dimension was 250 mm X 25 mm. The stress-strain curves for five specimens are shown in **Figure 2.** All specimens showed a similar trend consisting of a linear increase in stress with strain up to a peak where a brittle tearing took place. The average values of tensile strength, modulus, and failure strain with standard deviations inside the parenthesis are given in **Table 1.**

Table 1. Tensile properties of Formica sheet.

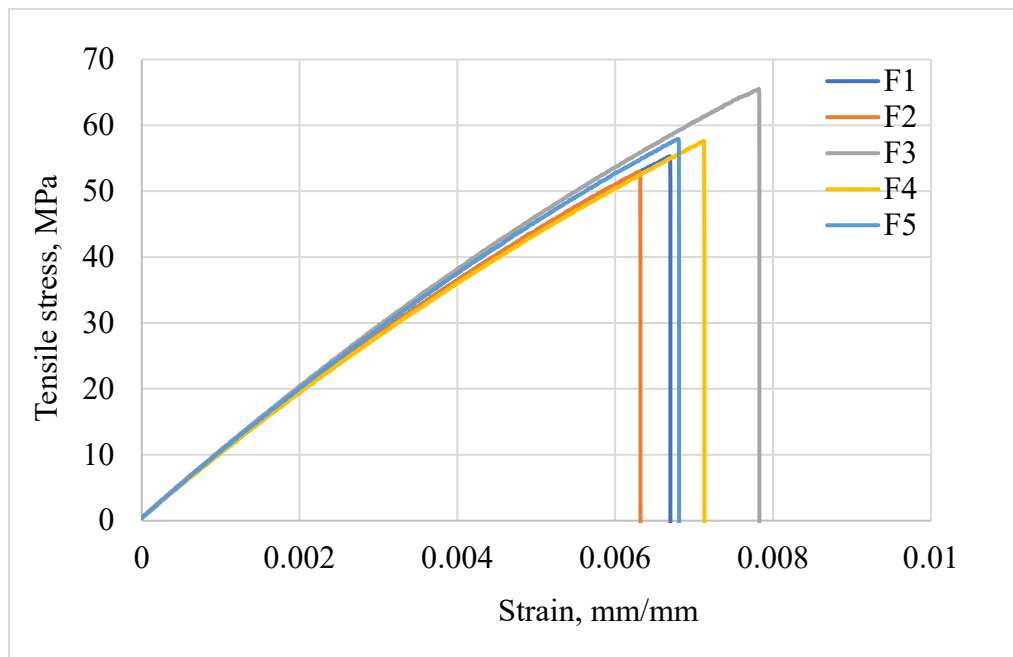| Sample	Tensile strength (MPa)	Tensile modulus (GPa)	Failure strain (%)
Formica sheet	57.89 (4.73)	8.91 (0.23)	0.69 (0.05)

Figure 2. Tensile stress-strain curves of Formica sheet.

Expanded perlite particles were purchased from Xinyang Caster New Material Co. Ltd., China. The particles were sorted into sizes between 2.36 mm to 4.75 mm using sieves to maintain uniformity. The powders and other sizes between 2.36 to 4.75 mm were filtered out. The expanded perlite contains 70-75% SiO_2, 12-16% Al_2O_3, 2.5-5% a_2O, 1-4% K_2O, 0.1-2% CaO, 0.15-1.5% Fe_2O_3, and 0.2-0.5% MaO, according to the manufacturer's catalog.

Sodium silicate solution (SSS) was supplied by Silica Solution, a concern of Rupam Soap & Chemical Industries Ltd., Bangladesh. The manufacturer's datasheet stated that the weight ratio of sodium oxide and silicon dioxide is 1:3.2 and a density of 1.381 g/cm^3 at 20°C. The solution contains 36.3±1.2 % of solid sodium silicate content (by weight). To vary the solid content further, the SSS was diluted with 10 % and 20 % drinking. The sample IDs and SSS dilution is shown in **Table 2**.

Table 2. Dilution of sodium silicate solution for different samples.

Sample ID	Sodium silicate solution, wt. %	Water, wt. %
FHCS-100, FCS-100	100	0
FHCS-90, FCS-90	90	10
FHCS-80, FCS-80	80	20

3.2. Specimen Preparation

3.2.1. Fabrication of Honeycomb Structure

The process of fabricating the sandwich structure consists of several steps such as paper honeycomb structure fabrication, perlite foam manufacturing, filling honeycomb cells, curing, and finally attaching skins. The hexagonal shape was chosen for the paper honeycomb to get better performance [32] and the paper honeycombs were fabricated by the traditional expansion process [33]. The fabrication process of the paper honeycomb structure is shown in **Figure 3**. Kraft paper was cut into strips of a width of 12 mm and a length of 320 mm using a paper cutter. Paper strips were marked as shown in **Figure 3(c)** with an interval of 20 mm. Glue (Fevicol SH) was applied to the strips at an interval of 20 mm and 20 strips were stacked together in such a way that the glued portion of one strip did not coincide with the adjacent one. After curing for 24 hours, the final step was to pull apart the strips to expand the stacked strips into a hexagonal honeycomb structure as shown in **Figure 3(e)**. The dimension of the honeycomb cells is shown in **Figure 3 (f).**
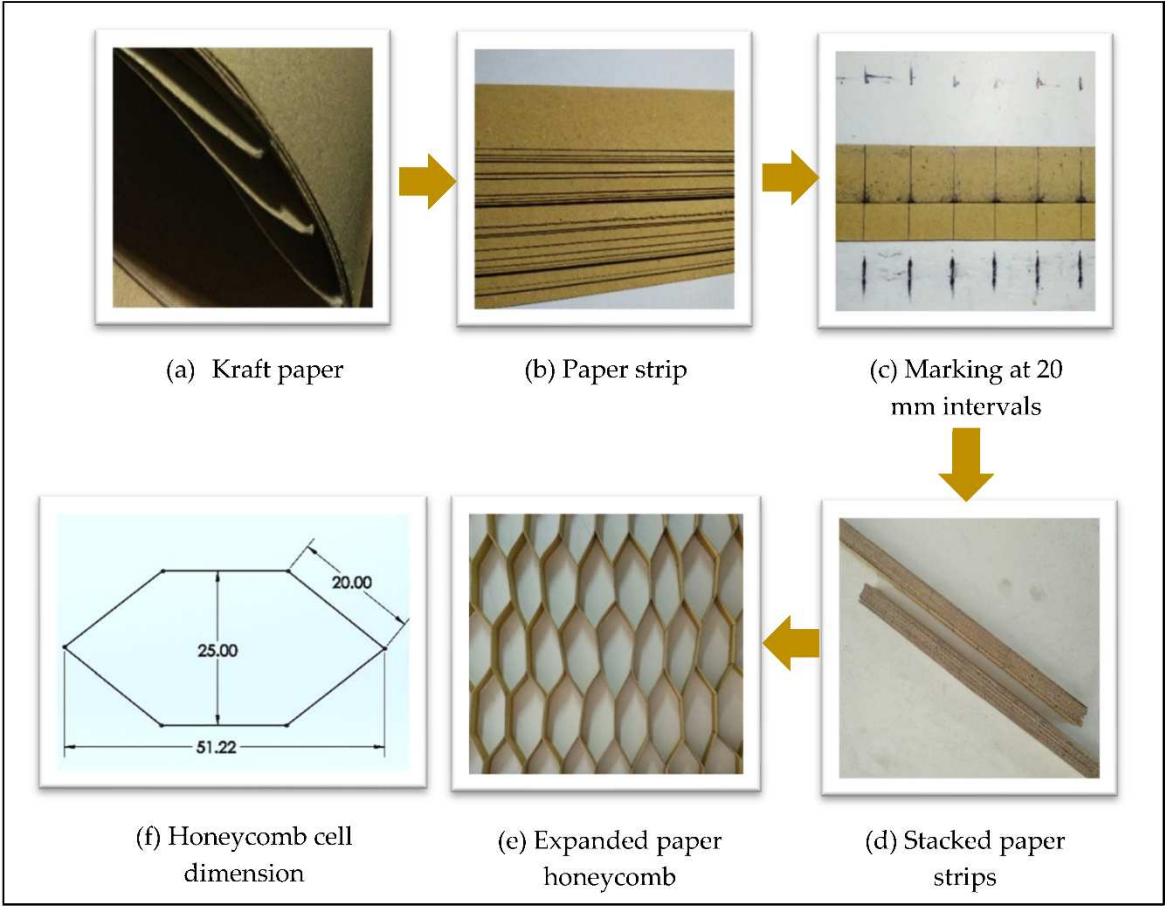
Figure 3. Fabrication process of the paper honeycomb structure.

3.2.2. Preparation of Perlite Foam Mixture

Figure 4 schematically shows the process of making the perlite/sodium silicate foam mixture. The SSS was diluted as presented in **Table 2**. Dry perlite particles were taken into a container and diluted SSS was poured into it followed by hand mixing for 5 minutes. The mixing proportion of the perlite, water, and sodium silicate solution for different samples is given in **Table 3**. A slightly higher amount of perlite particles were taken for manufacturing sandwich core without paper honeycomb to compensate for the density change. However, the total ratio of SSS to perlite particle was kept constant at 4.29.
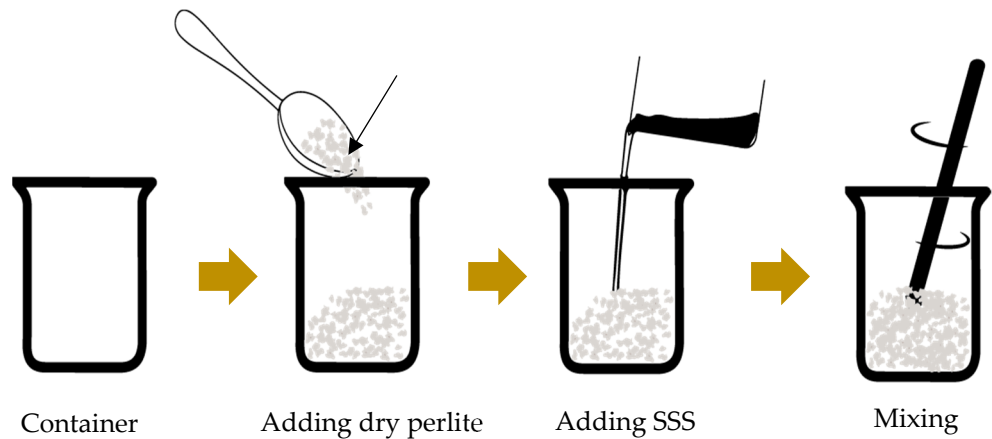

Figure 4. Steps for preparing perlite/sodium silicate foam mixture.

Table 3. Amount of the constituents for preparing perlite/sodium silicate foam mixture.

Sample ID	Mass of perlite (g)	Mass of SSS as received (g)	Mass of water (g)	Mass of diluted SSS (g)
FHCS-100	85	365.00	0	365.00
FCS-100	90	386.47	0	386.47
FHCS-90	85	328.50	36.50	365.00
FCS-90	90	347.82	38.65	386.47
FHCS-80	85	292.00	73.00	365.00
FCS-80	90	309.18	77.29	386.47

3.2.3. Core Manufacturing

The expanded honeycomb structure was placed into a mold of dimension 250 mm X 250 mm then the perlite/sodium silicate foam mixture was poured into the cells of the honeycomb structure manually. The top surface of the filled mold was made plain using a metal bar by applying light compaction. The wet foam-filled mold was then placed inside an electric oven at 80°C for 24 hours to cure. A load of approximately 4 kg was kept on the top of the wet foam-filled honeycomb to resist the bending of the core during curing. After curing the bottom surface of the core was found to be smooth and the paper honeycomb edges were visible but the top surface was rough and the paper honeycomb edges were not visible because some of the particles were broken and remained on top of the paper honeycomb when the compaction was applied using the metal bar. To ensure proper adhesion of the paper honeycomb edges with the sandwich skin, it was necessary to polish the top surface using emery paper to make the paper honeycomb edges visible. A photograph of the manufactured foam-filled paper honeycomb core is shown in **Figure 5 (a)**. For manufacturing perlite/sodium silicate foam without paper honeycomb, the wet mixture of the perlite and sodium silicate was poured into the mold and the top surface was leveled. After that, the curing process was the same as the foam-filled paper honeycomb cores.
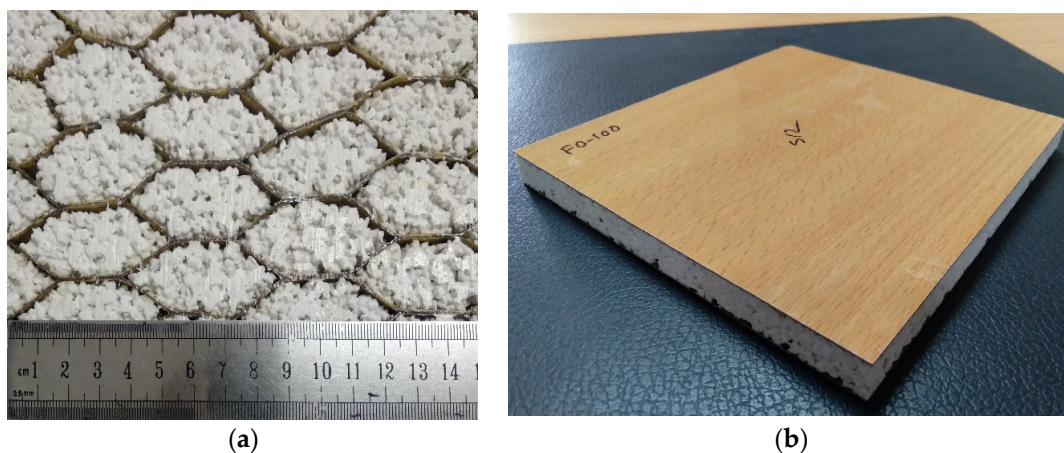

(a)   (b)

Figure 5. Typical photograph of (a) perlite/sodium silicate foam-filled paper honeycomb core and (b) sandwich structure made of perlite/sodium silicate foam core and Formica sheet as skin.

3.2.3. Fabrication of Sandwich

The Formica sheet was cut into a rectangular shape of 250 mm X 250 mm which was the internal size of the mold. The Formica sheet was attached to both surfaces of the core with 20 grams of adhesives on the rough surface of each sheet. The adhesive was evenly distributed using a brush. The Formica skin was attached keeping the longitudinal direction of the honeycomb cell aligned with the longitudinal direction of the Formica sheet. To minimize distortion, the sandwich specimens were further sandwiched between two flat glass plates, and a load of approximately 4 kg was placed above the top glass plate. The sandwich was left for additional 24 hours for the adhesive to cure. A typical photograph of the foam core sandwich without a paper honeycomb is shown in **Figure 5(b)**. The

sandwich structures were cut into 250 mm X 80 mm along the longitudinal direction using a circular saw.

3.3. Density Measurement

The length, width, and thickness were measured using digital slide calipers (Mitutoyo 0 - 300 mm, Japan) with an accuracy of 0.01 mm. The mass of the sample was measured using a weighing machine (AND Company Ltd., 0.01 - 300 g, Korea) with an accuracy of 0.01 g. The density of the samples was determined using the equation

$$\rho = \frac{M}{V},\tag{1}$$

where, ρ, M, and V are the density, mass, and volume of the specimen respectively.

3.4. Flexural Testing

Three-point bending tests were conducted in a universal testing machine (Shimadzu AGX-300kNV, Japan) at a crosshead speed of 6 mm/min and support span length of 150 mm according to standard ASTM C393/C393M-11 [34]. **Figure 6** shows a schematic diagram of the three-point bending test arrangement. The diameter of the loading roller and support rollers were 10 mm and 30 mm respectively. At least three specimens were tested for sandwiches with foam core only and six specimens were tested for sandwiches with foam-filled paper honeycomb core. The data (load and deflection) were recorded using the data acquisition software TrapeziumV by Shimadzu, Japan at an interval of 0.05 seconds. The ultimate core shear strength (F_s) and average facing strength (σ_{skin}) were calculated using Eqs. (2) and (3) respectively according to ASTM C393/C393M-11.

$$F_s = \frac{P}{(d+c)b} \text{ and} \tag{2}$$

$$\sigma_{skin} = \frac{PS}{2t(d+c)b} \tag{3}$$

where, P, S, b, d, t, and c are the applied load, support span length, specimen width, specimen depth, skin thickness, and core thickness respectively.
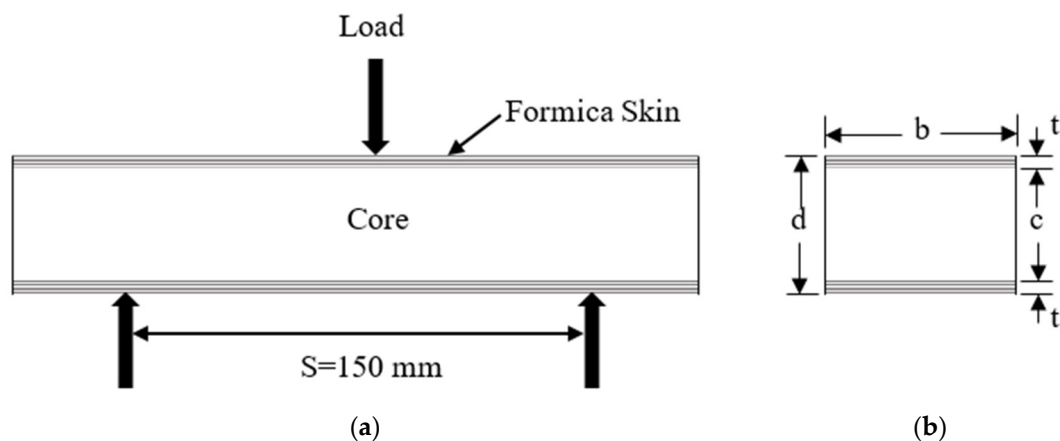

Figure 6. A schematic diagram of (a) flexural test setup and (b) dimension convention of the sandwich cross-section.

3.5. Thermal Conductivity Testing

Lee's disk method [35] is well known for measuring the thermal conductivity of the insulation material which was used to determine the thermal conductivity of the sandwiches. For the thermal conductivity test, the samples were cut into circular shapes with a diameter of 100 mm. **Figure 7**

shows the experimental setup for the thermal conductivity test. The following equation was used to determine the thermal conductivity:

$$k = \frac{mS\left(\frac{dT}{dt}\right)x}{A\,(\,T_2 - T_1)} \tag{4}$$

where, m, S, x, and A are the mass of the lower disk, the specific heat capacity of brass, the slope of the cooling curve, specimen thickness, and the area of the specimen respectively. The detailed procedure for measuring thermal conductivity using Lee's disc method can be found in Ref. [35].
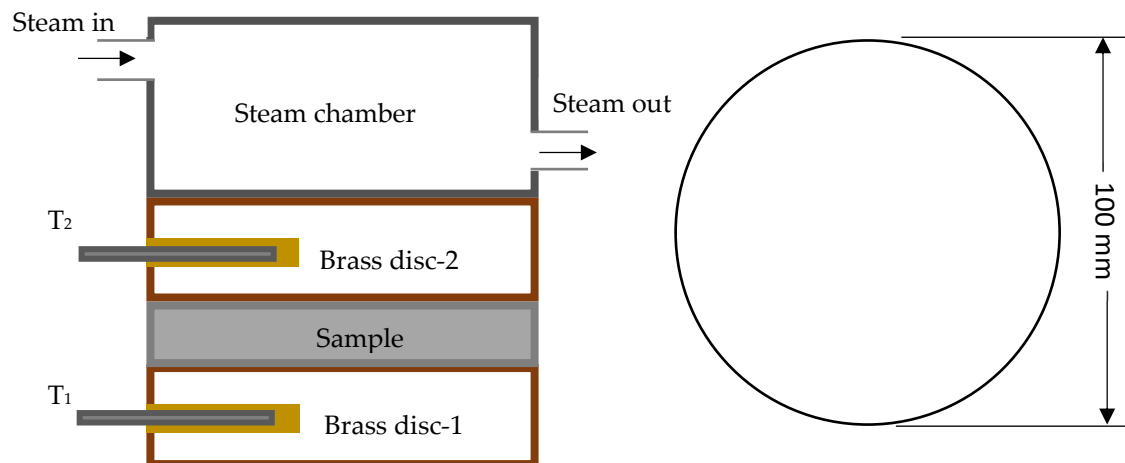

Figure 7. A schematic diagram of the thermal conductivity test setup.

4. Results and Discussion

4.1. Flexural Properties

The density, core shear stress, facing stress, flexural modulus, equivalent flexural strength, and thermal conductivity of different samples are given in **Table 4**. The densities of the prepared sandwiches are shown as a bar chart in **Figure 8** with standard deviation indicated by the error bars. The range of density of the sandwiches with and without paper honeycomb was found to be between 0.40 - 0.47 g/cm³. The density of the sandwiches appeared to be slightly decreasing with decreasing solid content in the SSS through dilution. Comparing the density of FHCSs and FCSs, the density of FCSs is slightly lower than the FHCSs although extra perlite was used in the FCSs. The insignificant deviation in density is favorable for comparing the mechanical properties of the sandwiches. For the sandwich with paper honeycomb core only, the density was found to be 0.15 g/cm³ which is 62.5 % lower than the lowest-density sandwich (e.g. FCS-80) in this study.

Table 4. Flexural characteristics of sandwich structures.

| Sample ID	Density, g/cm³	Core shear stress, MPa	Facing stress, MPa	Flexural modulus, GPa	Flexural strength, MPa	Thermal conductivity, W/mK
FHCS-100	0.47 ± 0.010	0.35 ± 0.10	51.26 ± 13.81	1.76 ± 0.09	11.03 ± 2.95	0.10 ± 0.010
FHCS -90	0.44 ± 0.003	0.27 ± 0.02	39.72 ± 3.00	1.61 ± 0.07	8.55 ± 0.64	0.11 ± 0.003
FHCS -80	0.42 ± 0.007	0.20 ± 0.06	28.64 ± 7.65	1.30 ± 0.09	6.26 ± 1.70	0.10 ± 0.010
FCS-100	0.46 ± 0.009	0.23 ± 0.05	33.69 ± 6.86	1.44 ± 0.09	7.79 ± 1.62	0.11 ± 0.010
FCS -90	0.43 ± 0.006	0.22 ± 0.03	31.53 ± 4.36	1.19 ± 0.14	7.45 ± 1.08	0.11 ± 0.010
FCS -80	0.40 ± 0.011	0.13 ± 0.03	18.95 ± 3.85	1.07 ± 0.21	4.06 ± 0.82	0.09 ± 0.004
HCS	0.15 ± 0.008	0.04 ± 0.02	4.59 ± 1.81	0.22 ± 0.12	1.01 ± 0.40	-
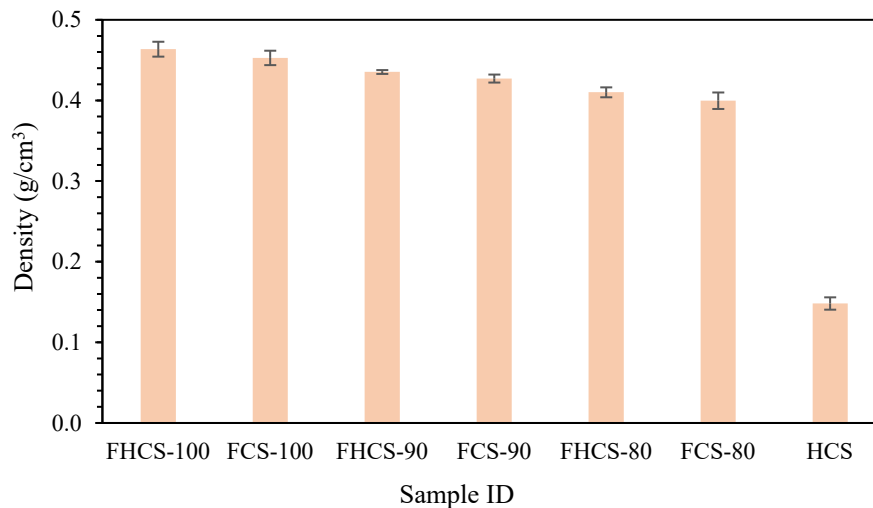
Figure 8. Density of various sandwich structures.

The flexural strength and modulus of the sandwich structures are shown in **Figure 9**. As expected, the flexural strength and modulus decreased with decreasing the concentration of solid content in the SSS due to dilution for both types of sandwiches (i.e. with and without paper honeycomb). The flexural strength and modulus of FHCSs were found to be higher than that of FCSs for each SSS concentration. The flexural strength of FHCSs increased by 41.65 %, 14.68 %, and 54.12% for SSS concentrations of 100 %, 90 %, and 80 % respectively compared to the respective FCSs. The improvement in flexural modulus of FHCSs was seen to be 22.05 %, 35.01 %, and 21.00 % for SSS concentrations of 100 %, 90 %, and 80 % respectively. The flexural strength of the HCS was found to be 1 MPa which is significantly lower than that of other sandwiches in this study. The flexural strength and modulus of the HCS increased considerably due to foam filling. The flexural strength of the FHCSs made by filling perlite/sodium silicate composite foams of 100 %, 90 %, and 80 % SSS concentrations increased by 998.85 %, 751.75 %, and 523.74 % respectively compared to HCS. The flexural modulus of the HCS increased by 734.66 %, 665.35 %, and 516.24 % due to filling with perlite/sodium silicate foams manufactured with 100 %, 90 %, and 80 % SSS concentrations respectively.
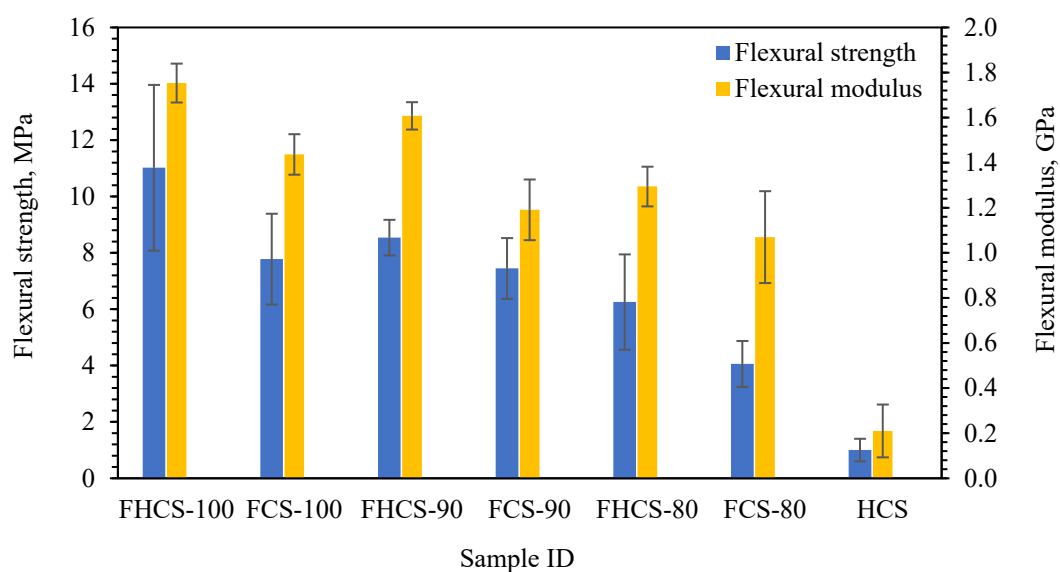

Figure 9. Flexural strength and modulus of various sandwich structures.

The facing stress developed in the sandwich structures during the flexural test is shown in **Figure 10**. For the sandwich structures irrespective of the honeycomb incorporation, it is seen that the sandwiches made of high SSS concentration showed higher facing stress. The reinforcement of paper honeycomb increased the facing stress of the sandwich structures by 52.19 %, 25.99 %, and 51.18 % for SSS concentrations of 100 %, 90 %, and 80% respectively. According to the results, FCS-80 showed the lowest facing stress of 18.94 MPa, and FHCS-100 showed the highest facing stress of 51.26 MPa. The facing stress increased from 4.59 MPa to a maximum of 51.26 MPa (increased by 1016.78 %) due to filling the paper honeycomb core-based sandwich (HCS) with perlite/sodium silicate foam made of 100% SSS. The improvements were 765.14 % and 523.75 % for the perlite/sodium silicate foams made of 90 % and 80 % SSS. The maximum facing stress developed in the FHCS-100 sandwich is 51.26 MPa which is 12.93 % less than the tensile strength (57.89 MPa as shown in **Table 1**) of the Formica sheet. Therefore it can be hypothesized that any sandwiches in this investigation under flexural loading must not fail by face sheet tearing at the tension side of the specimen. The failure modes of the sandwiches are discussed later in this paper.

The core shear stress at peak load for different samples is also shown in **Figure 10** in the secondary axis with standard deviations as error bars. Similar to the facing stress, the core shear stress decreased with the dilution of the SSS. The core shear stress developed in the FHCSs was also found to be higher than that of the corresponding FCSs. On the other hand, the HCS showed a core shear stress of 0.03 MPa, and the core shear stress also increased significantly similar to facing stress due to filling the HCS with perlite/sodium silicate foams.
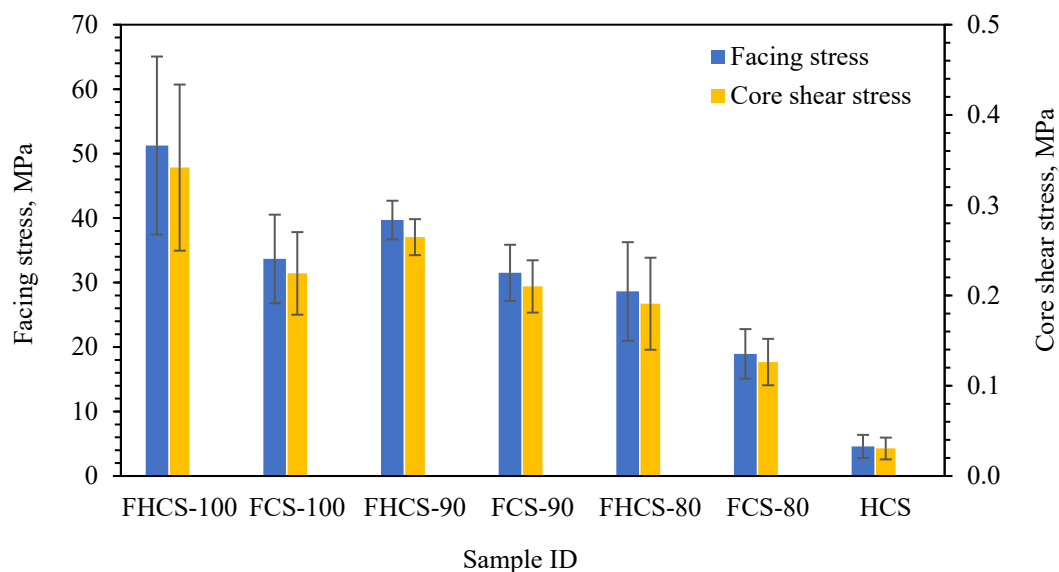

Figure 10. Facing stress and core shear stress of various sandwich structures.

Specific properties are very important for describing lightweight materials and they are given in **Table 5**. It can be seen from **Table 5** that the characteristic features of specific flexural properties are similar to that of general flexural properties (as discussed earlier) because of the insignificant change in densities of the sandwich structures with and without the paper honeycomb. However, the specific flexural properties of both FHCSs and FCSs appeared to be significantly higher than that of the HCS although the density of the HCS was considerably lower. For instance, the FHCS structure with 100 % SSS concentration exhibited a 251.11 % higher specific flexural strength compared to the HCS structure.

**Table 5.** Specific flexural properties of the sandwich structures in this study and from the literature.

Sample ID	Density (g/cm³)	Sp. flexural strength, [MPa/(g/cm³)]	Sp. flexural modulus, [GPa/(g/cm³)]
FHCS-100	0.47	23.77	3.78
FHCS-90	0.44	19.62	3.69
FHCS-80	0.42	15.25	3.16
FCS-100	0.46	17.18	3.17
FCS-90	0.43	17.44	2.79
FCS-80	0.40	10.15	2.68
HCS	0.15	6.77	1.42
Portland cement skin with kraft paper honeycomb core [25]	0.99	0.88	-
Flax-reinforced Portland cement skin with kraft paper honeycomb core [25]	0.89	1.74	-
Oriented strand boards or plywood [36]	0.55	29.82	8.97
Gypsum-fibre boards [36]	1.15	3.48	3.30
Chips board urea-formaldehyde bonded [37]	0.72	15.97	2.68
MDF [37]	0.68	27.50	-
Coconut coir cement board [38]	1.13	17.64	4.70
Commercial flake board [38]	1.40	8.43	4.29
Commercial cellulose board [38]	1.56	12.24	4.22
Gypsum panel [11]	1.00	2.26	2.12
Jute fiber reinforced gypsum panel [11]	0.97	2.03	2.24
Perlite/sodium silicate foam panel [21]	0.41	2.37	0.87
Syntactic foam panel [39]	0.37	21.32	2.86
Syntactic foam panel [39]	0.44	17.20	2.57
Nylon fiber reinforced perlite/sodium silicate panel [18]	0.41	2.68	0.61
Perlite/sodium silicate foam with jute fiber reinforced epoxy composite skin [30]	0.59	6.50	0.61

Table 5 also shows the specific flexural properties of some similar building materials reported in the literature. The specific flexural strength and modulus of the sandwiches developed in this work are significantly higher than similar building materials including Gypsum panels [11], gypsum fiber boards [36], and Plywood [36]. The density of building materials such as perlite/sodium silicate foam [21], syntactic foam [39], nylon fiber reinforced perlite sodium silicate foam [18], sandwich structure made perlite/sodium silicate foam core with jute fiber reinforced epoxy composite skin [30] reported in the literature falls within the density range of the sandwiches in this work but their specific flexural properties are comparatively lower than the sandwiches in this study. So, the developed sandwich structures may be a potential candidate for applications in the building of non-load-bearing structures.

4.2. Flexural Load-deflection Curves and Failure Mechanism

Typical load-deflection curves and photographs of the specimens showing the failure mode during the flexural test are given in **Figure 11 (**for FCSs**) and Figure 12** (for FHCSs). All curves showed a linear increase in load with deflection up to a peak where the failure was initiated. The failure modes for various sandwich structures under flexural loading are summarized in **Table 6**. The failure was initiated by core shear cracking for all FCSs and FHCSs irrespective of the SSS concentrations because of the low shear strength of the perlite/sodium silicate core. For FCS with 100% SSS concentration, the failure sequence was found to be core shear cracking [**Figure 11(b)-(ii)**] followed by a small delamination and top skin fracture [**Figure 11(b)-(iii)**] and for other FCSs, the failure sequence was the core shear cracking followed by the delamination of either top or bottom or both skins from the core. On the other hand, for all FHCSs the core shear cracking [**Figure 12(b)-(ii)**] was followed by the top skin fracture [**Figure 12(b)-(iii)**]. After careful observation of the recorded

video of the flexural testing and the corresponding load–deflection curves, the portion of the curves during shear cracking, skin delamination, and skin fracture were identified and shown in **Figure 11(a)** for FCSs and **Figure 12(a)** for FHCSs. It is observed from the load–deflection curves that the core shear and delamination caused a gradual drop in load with deflection whereas the skin fracture triggered a rapid drop in the load-bearing capacity of the sandwiches. In the case of HCS, it is seen that the load increased with increasing deflection up to a peak followed by a gradual drop in load with increasing deflection **Figure 11(a)** and **Figure 12(b)**. The local deformation of the top skin initiated at the peak load due to buckling of the paper honeycomb core as shown in **Figure 11(b)-(iv)**.
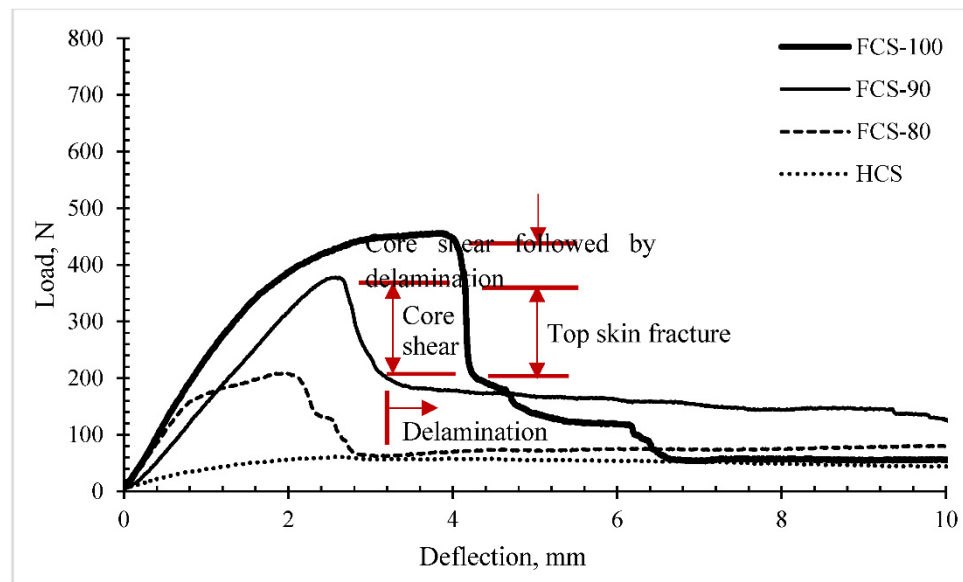
(**a**)
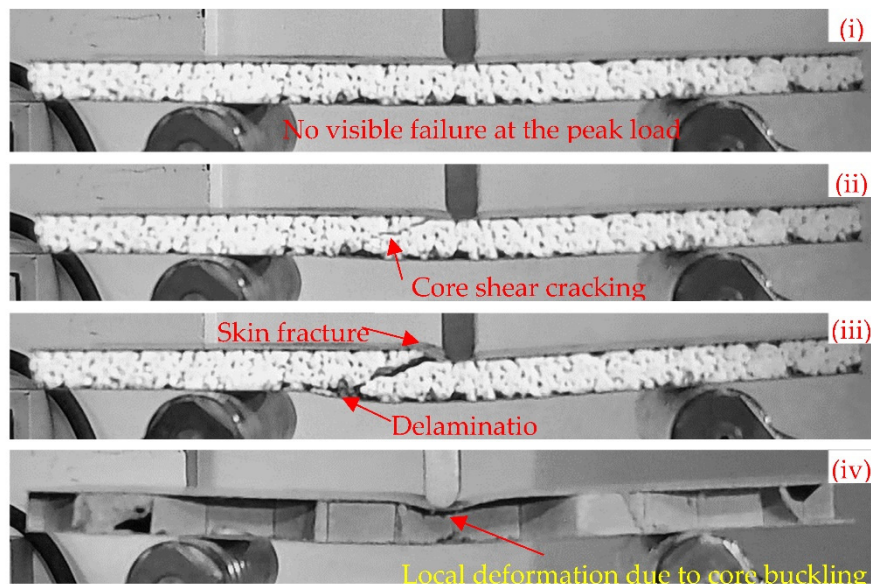
(**b**)

Figure 11. a) Typical load vs displacement curves of foam core-based sandwiches and (b) Typical photographs of the failed sandwiches during the flexural test.
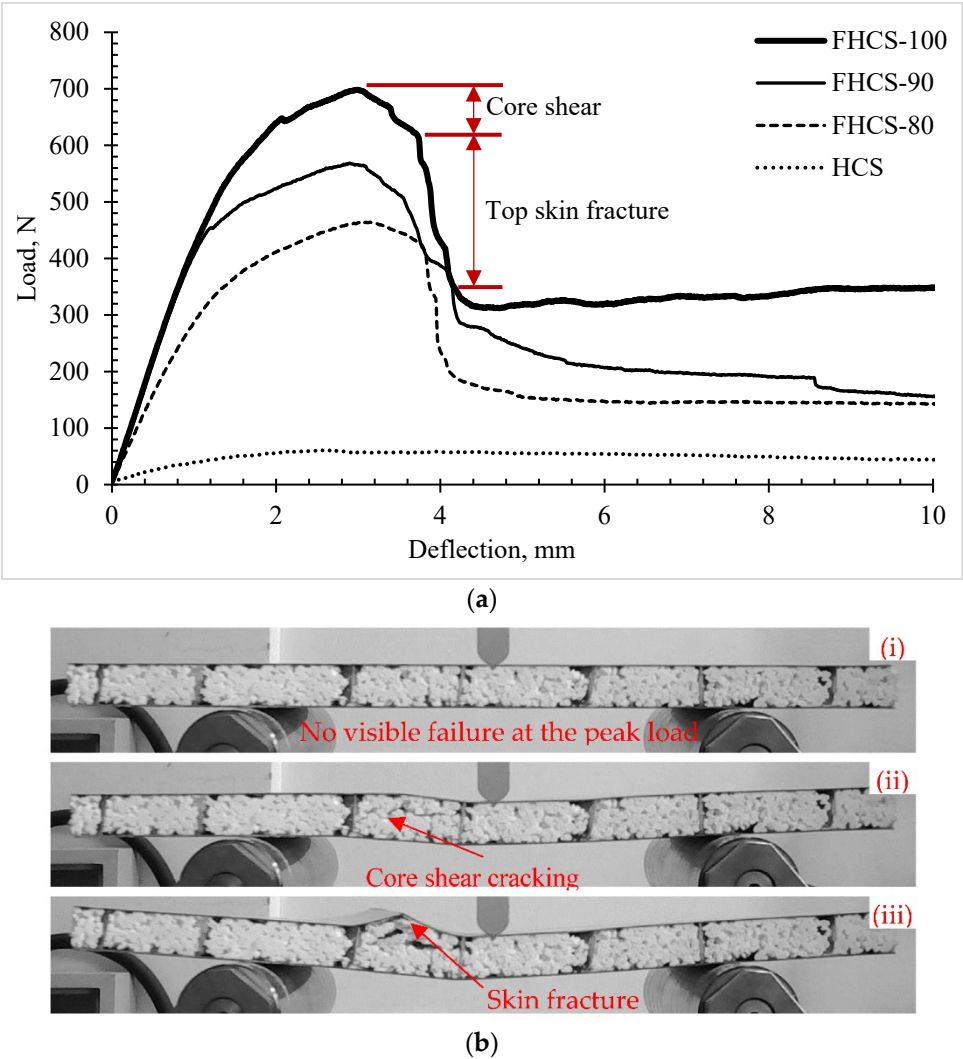
(**a**)

(**b**)

Figure 12. a) Typical load vs displacement curves of foam-filled honeycomb core-based sandwiches and (b) Typical photographs showing failure modes of the sandwich during the flexural test.

Table 6. Summary of the failure mechanisms of various sandwich structures.

Sample ID	Failure Sequence
FHCS - 100	Core shear – top skin fracture
FHCS - 90	Core shear – top skin fracture
FHCS - 80	Core shear – top skin fracture
FCS - 100	Core shear – delamination - top skin fracture
FCS - 90	Core shear – delamination
FCS - 80	Core shear – delamination
HCS	Local buckling of honeycomb core

A comparison of load–deflection curves for FHCS-100, FCS-100, HCS, and the summation of HCS and FCS-100 are given in Figure 13. It is seen that the load-bearing ability of FHCS is significantly higher than HCS, FCS-100, and both HCS and FCS-100 combined indicating a remarkably higher load-bearing capability of FHCSs due to interaction effect.
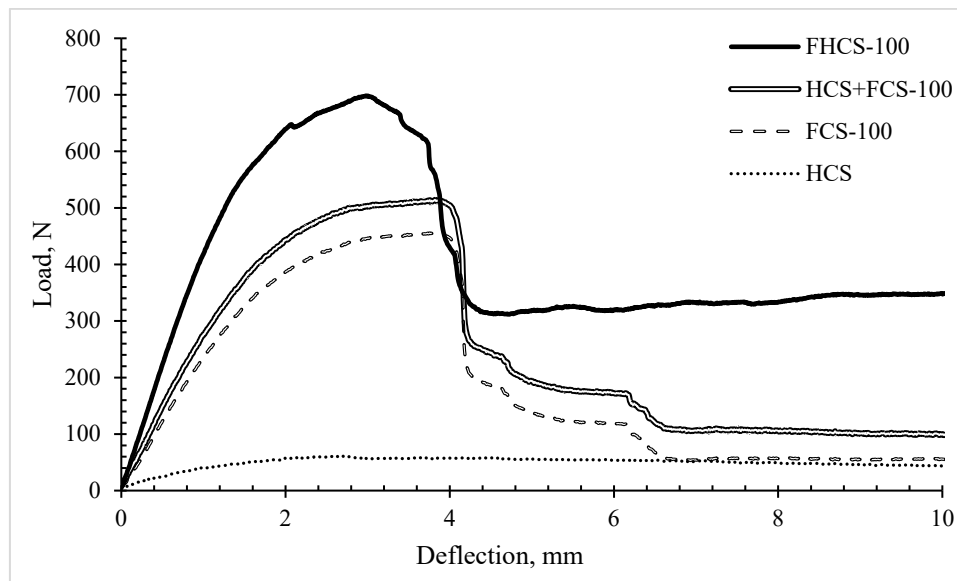
Figure 13. Comparison of load-deflection curves of HCS, FCS-100, the summation of HCS and FCS-100, and FHCS-100.

4.8. Thermal Behavior

The thermal conductivity of the different samples is shown in **Figure 14** with the standard deviation indicated by the error bars. The range of thermal conductivity of the sandwiches with and without paper honeycomb was found to be between 0.095 - 0.113 W/mK. It is clear from the figure that the effect of solid content in SSS and paper honeycomb reinforcement on thermal conductivity is insignificant.
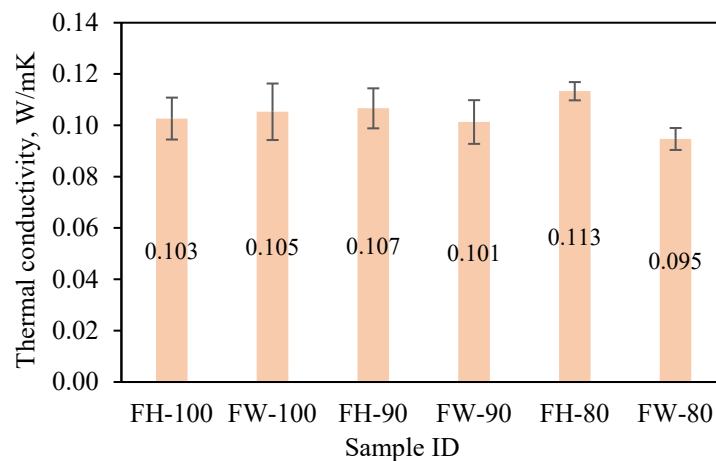

Figure 14. Thermal conductivity of different samples with standard deviations as error bar.

The thermal conductivities of various non-load-bearing building materials reported in the literature along with the results of the current study are given in **Table 7**. It is seen that the thermal conductivities of MDF [37], Plywood-Scots pine & Black pine [40], particleboard [37], flax reinforced Portland cement skin with kraft paper honeycomb core sandwich [25] falls within the range of thermal conductivity of the sandwiches reported in this work. However, it is interesting to see that the density of those materials is significantly higher than the sandwiches in this work. The densities of date palm waste-MDF sandwich panel [41], polystyrene foamed concrete [42], and cork-gypsum composite [43] are within the range of the densities of the sandwich panels in this study but their thermal conductivity is higher than the sandwiches developed in this work. So, the thermal conductivity of the sandwiches reported in this work has a high potential to be used as a non-load-

bearing building material because of their lower thermal conductivity combined with lightweight properties.

Table 7. Thermal conductivity of various building materials found in the literature along with the results of the current study.

Reference	Materials	Density(g/cm³)	Thermal Conductivity(W/m.K)
[25]	Gypsum Board	0.65	0.159
[36]	Gypsum fiberboard	1.15	0.32
[37]	MDF	0.696	0.0974
[37]	Thin MDF	0.802	0.1104
[41]	Date Palm Waste-MDF sandwich panel	0.456	0.1357
[36]	Oriented strand boards (OSB) or plywood (PWD)	0.65	0.13
[37]	Plywood (Beech)	0.679	0.1304
[40]	Plywood (Scots pine)	0.58	0.10
[40]	Plywood (Black pine)	0.60	0.11
[37]	Particleboard	0.597	0.0965
[25]	Flax-reinforced Portland cement skin with kraft paper honeycomb core	0.89	0.097
[38]	Coconut coir cement board	1.04	0.40
[38]	Commercial flakeboard	1.04	0.36
[38]	Commercial cellulose board	1.56	0.68
[42]	Polystyrene foamed concrete	0.4	0.157
[43]	Cork–gypsum composite	0.472	0.124
[44]	Gypsum composite	0.88	0.13
[45]	Newspaper sandwiched ALC panel	1.1	0.30
Current study	Perlite/sodium silicate foam-based sandwich with Formica sheet skin	0.40-0.47	0.095 - 0.113

5. Conclusions

Novel sandwich structures were manufactured with paper honeycomb, perlite/sodium silicate foam, and perlite/sodium silicate foam filled paper honeycomb as core with Formica sheet as skin. The flexural properties along with the failure mechanism and thermal conductivity of the manufactured sandwich structures were investigated. The findings of this work can be summarized as follows:

- The flexural properties of the foam-only sandwich structures improved significantly with the addition of paper honeycomb reinforcement, indicating a potential method for enhancing foam

core-based sandwich structures. Furthermore, the introduction of perlite/sodium silicate composite foam filling in the cells of the paper honeycomb core resulted in a remarkable increase in the flexural properties of the sandwich structures.

- The paper honeycomb core-based sandwich structure exhibited a reasonable flexural strength of 1.01 MPa, making it suitable for non-load-bearing structures. The density of the sandwich structures increased due to foam filling, but the specific flexural properties were substantially greater than the paper honeycomb core-based sandwiches.

- The failure initiation due to flexural loading in foam only and foam-filled paper honeycomb sandwich structures occurred by core shear cracking. In contrast, the failure in the paper honeycomb core-based sandwich was found to be local deformation due to core buckling.

- The highest facing stress developed in the sandwich structure was lower than the tensile strength of the Formica sheet indicating that the performance of the sandwich structures could be further improved by enhancing the shear strength of the core.

- Core shear failure did not significantly impact the load-bearing capacity of the sandwiches. Instead, the second stage of failure, such as delamination or skin fracture, led to a rapid drop in load-bearing capacity.

- The concentration of sodium silicate and the presence of paper honeycomb reinforcement in the perlite/sodium silicate foam core-based sandwich structures had an insignificant effect on thermal conductivity.

- The thermal conductivity of the foam core-based sandwiches, with and without paper honeycomb, ranged from 0.095 to 0.113 W/mK, which is significantly lower than that of many existing building materials described in the literature. Additionally, the specific flexural properties of the sandwiches studied in this work were comparable to those of common building materials used in non-load-bearing applications.

References

1. Berge, B., *The ecology of building materials*. 2009: Routledge.
2. Lanzón, M. and P. García-Ruiz, *Lightweight cement mortars: Advantages and inconveniences of expanded perlite and its influence on fresh and hardened state and durability.* Construction and Building Materials, 2008. **22**(8): p. 1798-1806.
3. Dube, W., L. Sparks, and A. Slifka, *Thermal conductivity of evacuated perlite at low temperatures as a function of load and load history.* Cryogenics, 1991. **31**(1): p. 3-6.
4. Ennis, D. *Perlite mining and reclamation in the no aqua peaks, Taos County, New Mexico.* in *62nd Field Conference Geology of the Tusas Mountains–Ojo Caliente: New, Mexico, USA, New Mexico Geological Society Guidebook.* 2011.
5. Yilmazer, S. and M.B. Ozdeniz, *The effect of moisture content on sound absorption of expanded perlite plates.* Building and Environment, 2005. **40**(3): p. 311-318.
6. Rashad, A.M., *A synopsis about perlite as building material–A best practice guide for Civil Engineer.* Construction and Building Materials, 2016. **121**: p. 338-353.
7. Jack, M. and C.E. Rahr, *Building board of fiber and asphalt coated perlite.* 1953, Google Patents.
8. Sherman, N. and J.H. Cameron, *Method of manufacturing improved mineral board.* 1981, Google Patents.
9. Shastri, D. and H.S. Kim, *A new consolidation process for expanded perlite particles.* Construction and Building Materials, 2014. **60**: p. 1-7.
10. Vimmrova, A., et al., *Lightweight gypsum composites: Design strategies for multi-functionality.* Cement and Concrete Composites, 2011. **33**(1): p. 84-89.
11. Karua, P., M. Arifuzzaman, and M.S. Islam, *Effect of jute fiber reinforcement on the mechanical properties of expanded perlite particles-filled gypsum composites.* Construction and Building Materials, 2023. **387**: p. 131625.
12. Arifuzzaman, M. and H.S. Kim, *Novel mechanical behaviour of perlite/sodium silicate composites.* Construction and Building Materials, 2015. **93**: p. 230-240.
13. Arifuzzaman, M. and H.S. Kim. *Flatwise Compression and Flexural Behaviour of Perlite/Sodium Silicate Composite Foam.* in *Applied Mechanics and Materials.* 2017. Trans Tech Publ.
14. Arifuzzaman, M. and H.S. Kim, *Prediction and evaluation of density and volume fractions for the novel perlite composite affected by internal structure formation.* Construction and Building Materials, 2017. **141**: p. 201-215.

15. Arifuzzaman, M. and H.S. Kim, *Plane Stress/Strain Compressive Behavior of Perlite Composite Foam.* Journal of Testing and Evaluation, 2019. **47**(4): p. 2905-2925.

16. Adhikary, P., M. Arifuzzaman, and E. Kabir, *Compressive properties of expanded perlite based particulate composite for the application in building insulation Board.* Journal of Engineering Advancements, 2020. **1**(1): p. 01-05.

17. Karua, P. and M. Arifuzzaman, *Compressive behavior of perlite/sodium silicate composite foam modified by boric acid.* Metallurgical and Materials Engineering, 2022. **28**(1): p. 103-124.

18. Takey, A.A.N., et al., *Effect of Nylon Fiber Reinforcement on Mechanical Behavior of Expanded Perlite/Sodium Silicate Composites*, in *2nd International Conference on Mechanical Engineering and Applied Sciences (ICMEAS)*. 2022, MIST: Dhaka, Bangladesh.

19. Tian, Y.L., et al., *A study of effect factors on sodium silicate based expanded perlite insulation board strength.* Applied Mechanics and Materials, 2013. **405**: p. 2771-2777.

20. Al Abir, A., M.O. Faruk, and M. Arifuzzaman. *Novel expanded perlite based composite using recycled expanded polystyrene for building material applications*. in *International Conference on Mechanical, Industrial and Energy Engineering*. 2020.

21. Arifuzzaman, M. and H.S. Kim, *Novel flexural behaviour of sandwich structures made of perlite foam/sodium silicate core and paper skin.* Construction and Building Materials, 2017. **148**: p. 321-333.

22. Wang, D., *Impact behavior and energy absorption of paper honeycomb sandwich panels.* International Journal of Impact Engineering, 2009. **36**(1): p. 110-114.

23. Dongmei, W., *Cushioning properties of multi-layer corrugated sandwich structures.* Journal of Sandwich Structures & Materials, 2009. **11**(1): p. 57-66.

24. Chen, Z. and N. Yan, *Investigation of elastic moduli of Kraft paper honeycomb core sandwich panels.* Composites Part B: Engineering, 2012. **43**(5): p. 2107-2114.

25. Shahbazi, S., et al., *Cementitious Insulated Drywall Panels Reinforced with Kraft-Paper Honeycomb Structures.* Buildings, 2022. **12**(8): p. 1261.

26. Fu, Y. and P. Sadeghian, *Flexural and shear characteristics of bio-based sandwich beams made of hollow and foam-filled paper honeycomb cores and flax fiber composite skins.* Thin-Walled Structures, 2020. **153**: p. 106834.

27. Abd Kadir, N., et al. *Experimental study on energy absorption of foam filled kraft paper honeycomb subjected to quasi-static uniform compression loading*. in *IOP Conference Series: Materials Science and Engineering*. 2016. IOP Publishing.

28. Abd Kadir, N., et al. *Experimental study of low-velocity impact on foam-filled Kraft paper honeycomb structure*. in *IOP Conference Series: Materials Science and Engineering*. 2018. IOP Publishing.

29. Safarabadi, M., et al., *Experimental and numerical study of buckling behavior of foam-filled honeycomb core sandwich panels considering viscoelastic effects.* Journal of Sandwich Structures & Materials, 2021. **23**(8): p. 3985-4015.

30. Sarkar, S.T., A.S.M. Aziz Naser; Ahammad, Raju; Islam, Md Shariful; Arifuzzaman, Md, *Mechanical behavior of sandwich structure made of perlite foam core and JFRP skin*, in *7th International Conference on Mechanical, Industrial and Energy Engineering (ICMIEE2022)*. 2022, Faculty of Mechanical Engineering, Khulna University of Engineering & Technology: Khulna, Bangladesh. p. ICMIEE22-212-1-5.

31. Hossain, G.M.I.K., Pranto; Arifuzzaman, Md, *Mechanical Characterization of Novel Sandwich Structures Made of Perlite/Epoxy Core with JFRP Facings*, in *7th International Conference on Engineering Research, Innovation and Education (ICERIE2023)*. 2023, School of Applied sciences & Technology, SUST: Sylhet, Bangladesh. p. 341-1-7.

32. Zenkert, D., *An Introduction to Sandwich Structures, Student Edition.* Dan Zenkert, 2005. **110**.

33. Pflug, J., et al. *Continuously produced honeycomb cores*. in *INTERNATIONAL SAMPE SYMPOSIUM AND EXHIBITION*. 2003. SAMPE; 1999.

34. C393/C393M-11, A. *Standard Test Method for Core Shear Properties of Sandwich Constructions by Beam Flexure*. 2016.

35. Barragán, V., et al., *Testing a simple Lee's disc method for estimating throuh-plane thermal conductivity of polymeric ion-exchange membranes.* International Journal of Heat and Mass Transfer, 2022. **184**: p. 122295.

36. Casagrande, D., P. Grossi, and R. Tomasi, *Shake table tests on a full-scale timber-frame building with gypsum fibre boards.* European Journal of Wood and Wood Products, 2016. **74**: p. 425-442.

37. Thoemen, H., *Wood-based panels: an introduction for specialists*. 2010: Brunel University Press.

38.   Asasutjarit, C., et al., *Development of coconut coir-based lightweight cement board.* Construction and Building Materials, 2007. **21**(2): p. 277-288.

39.   Islam, M.M. and H.S. Kim, *Sandwich composites made of syntactic foam core and paper skin: Manufacturing and mechanical behavior.* Journal of Sandwich Structures & Materials, 2012. **14**(1): p. 111-127.

40.   Demirkir, C., et al., *Influence of aging procedure on bonding strength and thermal conductivity of plywood panels.* ACTA PHYSICA POLONICA A, 2016. **129**(6): p. 1230-1234.

41.   Haseli, M., M. Layeghi, and H.Z. Hosseinabadi, *Characterization of blockboard and battenboard sandwich panels from date palm waste trunks.* Measurement, 2018. **124**: p. 329-337.

42.   Sayadi, A.A., et al., *Effects of expanded polystyrene (EPS) particles on fire resistance, thermal conductivity and compressive strength of foamed concrete.* Construction and building materials, 2016. **112**: p. 716-724.

43.   Cherki, A.-b., et al., *Experimental thermal properties characterization of insulating cork–gypsum composite.* Construction and building materials, 2014. **54**: p. 202-209.

44.   San-Antonio-González, A., et al., *Lightweight material made with gypsum and extruded polystyrene waste with enhanced thermal behaviour.* Construction and Building Materials, 2015. **93**: p. 57-63.

45.   Ng, S.-C. and K.-S. Low, *Thermal conductivity of newspaper sandwiched aerated lightweight concrete panel.* Energy and Buildings, 2010. **42**(12): p. 2452-2456.